APPLICATION OF NON-SQUARE MATRIX GENERATED FROM ALGEBRAIC POLYNOMIAL IN MODELLING MORTALITY RATE INTENSITY

GBENGA MICHAEL OGUNGBENLE[1], ANTHONY CHUKWUEMEKA ONYEKONWU[2] AND AMINA HAMZA[3]

Abstract

Accurate modeling of age-specific mortality is crucial for actuarial applications, public health planning, and demographic forecasting. Traditional parametric models, such as Gompertz and Makeham laws, often fail to capture complex or nonlinear mortality patterns, particularly at early and advanced ages. This study proposes a novel approach to mortality modeling using non-square matrices generated from McCutcheon's polynomial, enabling flexible estimation of mortality rate intensities across diverse age cohorts. Three polynomial-based models were developed and applied to synthetic and empirical data to examine survival probabilities, instantaneous death rates, and the force of mortality. The results demonstrate that the non-square polynomial approach captures intricate age-specific mortality dynamics, including local kinks and oscillations, while providing smoother, more interpretable curves than conventional methods. The models reveal key features such as minimal mortality points, constant-force intervals, and accelerated mortality at senescent ages, offering improved predictive accuracy and scalability. This framework provides a robust tool for actuaries, demographers, and public health planners, facilitating enhanced life insurance pricing, pension fund evaluation, and demographic forecasting. The findings highlight the potential of extending classical mortality models with polynomial matrices to accommodate complex population dynamics and nonlinear mortality trends.

Keywords: Distribution, Mortality intensities, Survival functions, Non-parametric, Probability**.**

---

[1] Lecturer, Department of Actuarial Science, Faculty of Management Sciences, University of Jos, Nigeria

[2] Research Fellow, National Mathematical Centre Abuja, Nigeria

[3] Research Scientist, Department of Mathematics, Faculty of Science, University of Maiduguri, Nigeria

Introduction

Recent evolution and robust product design innovations in the life insurance market have continually drawn the attention of actuaries to mortality as a tradable risk through mortality-linked insurance products. This has heightened the need for accurate modelling and forecasting of mortality rates. Analytical modelling of mortality trends is particularly important due to its central role in life insurance underwriting, pension scheme management, and the broader study of population dynamics (Li, O'Hare, & Vahid, 2016).

Accurate mortality forecasting is essential for effective resource allocation and forward planning in insurance and pension systems (Bolx-Postigo, Aguero, & Melus-Moreno, 2019; Spreeuw, Owadally, & Kashif, 2022). Inadequate mortality estimation contributes significantly to longevity risk, which creates complex challenges in premium pricing, reserving, forward funding, and retirement planning. Life tables summarise survival probabilities and mortality experiences of a cohort and provide instantaneous mortality rates and probabilities of death as functions of age. These probabilities play a pivotal role in premium rating and reserving decisions in life insurance.

However, crude mortality rates derived from cohort data are subject to random fluctuations due to sampling variability. Consequently, smoothing techniques are required to remove random errors associated with observed mortality data. Life tables are therefore computationally intensive to construct, particularly when estimating present values of pension funds and insurance provisions (Ah-Khaliludin, Khalid, & AbdRahman, 2019).

Mortality data often exhibit clustering of deaths at infancy and advanced ages, while increasing steadily at intermediate ages. This characteristic leads to pooling deaths into age intervals, resulting in abridged life tables. Nevertheless, since deaths occur continuously, there is a growing need to estimate single-age mortality intensities rather than interval-based rates. Interpolation and smoothing techniques enable actuaries to derive instantaneous mortality intensities from abridged data.

One of the most critical challenges in mortality modelling lies in estimating mortality intensity functions, defined as the instantaneous rate of mortality at a given age. Although the true mortality intensity function is unknown, it can be approximated using observed mortality data. However, discrepancies between observed and estimated mortality rates may be substantial.

To address these challenges, previous studies have applied a range of smoothing and interpolation techniques. Li, O'Hare, and Vahid (2016) used Legendre polynomials, while Ah-Khaliludin et al. (2019) employed Akima's interpolation technique, which uses piecewise cubic polynomials to ensure smooth transitions across age intervals. Other non-parametric approaches including kernel smoothing, B-splines, smooth splines, isotonic regression, and wavelets have also been extensively discussed in the literature (Faraway, 2016; Oirov, Terbish, & Dorj, 2021; Kaishev et al., 2016).

While parametric mortality models are widely used, they impose restrictive functional forms that may fail to capture complex or irregular mortality patterns. The reliance on assumed distributions and expert judgement introduces potential model misspecification, highlighting a methodological gap in mortality intensity estimation.

McCutcheon's polynomial has long been applied in actuarial science to approximate age-specific mortality and survival functions. Extending this approach through the use of non-square matrix representations offers a flexible framework for modelling mortality intensity across varying age groups, cohorts, and time periods, particularly when data dimensions are unbalanced.

Objective

The objective of this paper is to develop and evaluate a flexible mortality intensity modelling framework using McCutcheon's polynomial and non-square matrix representations to improve the estimation of age-specific mortality rates.

Data and Methods

McCutcheon's polynomial is often used in the context of actuarial science and mortality rate modeling, particularly when dealing with mortality tables or cohort-based analysis. The application of a non-square matrix generated from McCutcheon's polynomial in modeling mortality rate intensity is a more advanced topic that combines actuarial techniques with matrix algebra for representing and solving mortality rate patterns. McCutcheon's polynomial is typically used to model the relationship between the age of an individual and the probability of survival or mortality rate. The polynomial gives a smooth curve that approximates mortality or survival functions, often used in mortality tables. In many mortality models, we approximate the mortality rate μ_x at age x with a polynomial expression such as:

$$\mu_x = \beta_0 + \beta_1 x + \beta_2 x^2 + \beta_3 x^3 + \ldots + \beta_k x^k \quad (1)$$

where β_i are the coefficients, and k is the degree of the polynomial, determining the complexity of the curve. A non-square matrix in this context would generally be a matrix where the number of rows and columns are not equal. Non-square matrices can arise in actuarial modeling when we have a model involving multiple cohorts or different periods, and the data structure doesn't necessarily align in a square form (i.e., age groups or cohorts may differ in size, which results in matrices that are not square). In mortality modeling, the use of a non-square matrix might arise when the model requires tracking mortality rates over multiple time periods (e.g., cohorts over years) or across multiple age groups (i.e., not all age groups have the same number of data points).

This non-square matrix could represent coefficients, adjustments or even rates for mortality intensities across varying parameters like age and time. In this case, the non-square matrix could be used to represent the coefficients or values of the polynomial (McCutcheon's polynomial) across different age cohorts and time periods. For example, we might use a matrix to store mortality rates at different ages for different time periods or different groups as follows.

$$M = \begin{pmatrix} \mu_1(\xi_1) & \mu_1(\xi_2) & \mu_1(\xi_3) & . & . & . & \mu_1(\xi_k) \\ \mu_2(\xi_1) & \mu_2(\xi_2) & \mu_2(\xi_3) & . & . & . & \mu_2(\xi_k) \\ \mu_3(\xi_1) & \mu_3(\xi_2) & \mu_3(\xi_3) & . & . & . & \mu_3(\xi_k) \\ . & . & . & . & . & . & . \\ . & . & . & . & . & . & . \\ . & . & . & . & . & . & . \\ \mu_n(\xi_1) & \mu_n(\xi_2) & \mu_n(\xi_3) & . & . & . & \mu_n(\xi_k) \end{pmatrix}$$

(1a)

where

M is a non-square matrix.

$\mu_n(\xi_k)$ represents the mortality rate at age group mmm at time ξ_k

n could represent a specific cohort, and ξ_k could be a year.

This matrix can then be multiplied with the polynomial coefficients to predict or adjust mortality intensities for each age group and time period. Mortality intensity is defined as the instantaneous rate of mortality, often represented by the force of mortality, μ_x which is related to survival and mortality probabilities. In a McCutcheon's polynomial model, you might have:

$$\mu_x = \sum_{j=0}^{k} \beta_j x^j$$

(1b)

If you apply this polynomial to the matrix M you are essentially fitting the polynomial over the data points in the matrix to estimate the mortality rate over time or across different age groups. By solving this system, you can track the mortality rate over a specified range of ages or cohorts, enabling predictions of future mortality or analysis of past trends.

Cohort-Specific Mortality Rates: If you have mortality rates for multiple cohorts over time, the matrix could be used to track these rates, with the non-square nature accommodating differences in the number of cohorts and time periods. Dynamic Mortality Models: In more advanced actuarial models, mortality rates can evolve over time. A non-square matrix could

be used to capture the changing nature of mortality rates across different time periods and age groups.

Multivariate Mortality Analysis: In cases where multiple factors influence mortality (e.g., socioeconomic status, lifestyle, geographic location), a non-square matrix could

Mathematical Preliminaries

Let (x) denote a life aged x where $x > 0$. Since the death of (x) can occur at any age $y \geq x$, the future lifetime of (x) can be modelled by the continuous complete future life time function T_x such that the true function of the mortality intensity at age x is given

$$\mu_x = \lim_{\Delta x \to 0+} \frac{1}{\Delta x} \mathrm{P}\left[T_x \leq \Delta x\right] \tag{1c}$$

$${}_{\xi}p_x = \exp\left\{-\int_x^{x+\xi} \mu_\theta d\theta\right\} \cong \exp\left\{-\sum_{\theta=x}^{x+\xi} \mu_\theta\right\} \tag{2}$$

where ${}_{\xi}p_x$ is the probability that individual (x) survives to age $x+\xi$

The problem of estimating death rate μ_x at any given instant occurs most often in mortality analysis. If l_x defines the expected number of lives surviving to age x and μ_x is the instantaneous death rate, then it is possible to evaluate the value of μ_x numerically from the first order ordinary differential equation described by

$$\mu_{x+\xi} l_{x+\xi} = -\frac{dl_{x+\xi}}{d\xi} \tag{3}$$

where

$$l_x = \int_0^\infty \mu_{x+\xi} l_{x+\xi} d\xi \tag{4}$$

Theorem

Let the random life time of a new born take value in the interval $[0,\infty)$, then

$$dF_X(x) = \mathbf{P}_0 \times dH(x) + \overline{f}_X(x)dx \tag{5}$$

where $\overline{f}_X(x)$ is the defective death density.

Proof

Let x define the age of a life with $x \geq 0$. The survival function l_x represents the survival probability from age 0 to age x. It is functionally connected with the death density function $f_X(x)$ as follows:

$$-f_X(x) = \frac{dl_x}{dx} \tag{5a}$$

$$l_x = \int_x^\infty f_X(t)dt = 1 - \int_0^x f_X(t)dt \tag{5b}$$

and force of mortality is given by

$$\mu_x = \frac{f_X(x)}{l_x} \tag{5c}$$

for all x such that $l_x > 0$

Observe that the distribution function of death $F_X(x) = 0$ for $x < 0$ and $F_X(0) = \mathbf{P}(X = 0)$ for $x > 0$

$$F_X(x) = \mathbf{P}(X \le x) = \mathbf{P}(0 \le X \le x) \tag{6}$$

$$\mathbf{P}(0 \le X \le x) = \mathbf{P}(X = 0) + \mathbf{P}(0 < X \le x) \tag{7}$$

Assume that the distribution function $F_X(x)$ is differentiable on $(0, \infty)$, then there exists a defective death density function $\overline{f}_X(x)$, $x > 0$ such that

$$F_X(x) - F_X(0) = \int_{-\infty}^{x} \overline{f}_X(\zeta)\, d\zeta \tag{8}$$

Define the Heavy side function

$$H(x) = \begin{cases} 1 & if \quad x \ge 0 \\ 0 & if \quad x < 0 \end{cases} \tag{9}$$

Then for all $x \in \mathbf{R}$, we observe that for $\mathbf{P}_0 = \mathbf{P}(X = 0)$

$$F_X(x) = \mathbf{P}_0 \times H(x) + \int_{-\infty}^{x} \overline{f}_X(\zeta) 1_{\{\zeta > 0\}}\, d\zeta \tag{10}$$

Now observe that

$$dH(x) = \delta(x)\, dx \tag{11}$$

$$dF_X(x) = \mathbf{P}_0 \times dH(x) + \overline{f}_X(x)dx \tag{12}$$

Hence the proof

Theorem

Let T_x be the random life time of a life aged x, then the curve of death function $l_\tau \mu_\tau$ is given by

$$\mu_x \times \int_0^\infty l_{x+s}\mu_{x+s}ds = l_0 \times \int_{-\infty}^\infty f_{T_0}(x)H'(x)dx \tag{13}$$

Proof

$$f_{T_x}(\tau) = ({}_\tau p_x) \times \mu_{x+\tau} \tag{14}$$

$$f_{T_0}(\tau) = ({}_\tau p_0) \times \mu_\tau = \frac{l_\tau \mu_\tau}{l_0} \tag{15}$$

$$\int_{-\infty}^\infty f_{T_0}(\tau)H'(\tau)d\tau = \lim_{s\to\infty}\left(\int_{-s}^{s} f_{T_0}(\tau)H'(\tau)d\tau\right) \tag{16}$$

$$\int_{-\infty}^\infty f_{T_0}(\tau)H'(\tau)d\tau = \lim_{s\to\infty}\left(\left[f_{T_0}(\tau)H(\tau)\right]_{-s}^{s} - \int_{-s}^{s} f'_{T_0}(\tau)H(\tau)d\tau\right) \tag{17}$$

$$\int_{-\infty}^\infty f_{T_0}(\tau)H'(\tau)d\tau = \left(\lim_{s\to\infty}\left[f_{T_0}(s)H(s) - f_{T_0}(-s)H(-s)\right] - \lim_{s\to\infty}\int_{-s}^{s} f'_{T_0}(\tau)H(\tau)d\tau\right) \tag{18}$$

$$\int_{-\infty}^{\infty} f_{T_0}(\tau) H'(\tau) d\tau = \lim_{s\to\infty} f_{T_0}(s) H(s) - \lim_{s\to\infty} f_{T_0}(-s) H(-s) - \lim_{s\to\infty} \int_{-s}^{s} f'_{T_0}(\tau) H(\tau) d\tau$$

(19)

From equation (9), $H(-s) = 0$

$$\int_{-\infty}^{\infty} f_{T_0}(\tau) H'(\tau) d\tau = \lim_{s\to\infty} f_{T_0}(s) - 0 - \lim_{s\to\infty} \left\{ \int_{-s}^{0} f'_{T_0}(\tau) H(\tau) d\tau + \int_{0}^{s} f'_{T_0}(\tau) H(\tau) d\tau \right\}$$

(20)

$$\int_{-\infty}^{\infty} f_{T_0}(\tau) H'(\tau) d\tau = \lim_{s\to\infty} f_{T_0}(s) - \lim_{s\to\infty} \left\{ 0 + \int_{0}^{s} f'_{T_0}(\tau) d\tau \right\}$$

(21)

$$\int_{-\infty}^{\infty} f_{T_0}(\tau) H'(\tau) d\tau = \lim_{s\to\infty} f_{T_0}(s) - \lim_{s\to\infty} \left[f_{T_0}(\tau) \right]_0^s$$

(22)

$$\int_{-\infty}^{\infty} f_{T_0}(\tau) H'(\tau) d\tau = \lim_{s\to\infty} f_{T_0}(s) - \lim_{s\to\infty} \left[f_{T_0}(s) - f_{T_0}(0) \right]$$

(23)

$$\int_{-\infty}^{\infty} f_{T_0}(\tau) H'(\tau) d\tau = f_{T_0}(0)$$

(24)

$$\int_{-\infty}^{\infty} f_{T_0}(\tau) H'(\tau) d\tau = \left({}_{\tau} p_0 \right) \times \mu_{\tau} = \frac{l_{\tau} \mu_{\tau}}{l_0}$$

(25)

$$l_{\tau} \mu_{\tau} = l_0 \times \int_{-\infty}^{\infty} f_{T_0}(\tau) H'(\tau) d\tau$$

(26)

replacing τ by x in (26) and observe that $l_x = \int_0^\infty l_{x+s}\mu_{x+s}ds$ in (4), we have

$$\mu_x \times \int_0^\infty l_{x+s}\mu_{x+s}ds = l_0 \times \int_{-\infty}^{\infty} f_{T_0}(x)H'(x)dx$$

(26a)

Hence the proof

McCutcheon (1981-1983) defines the force of mortality as

$$\mu_x = \frac{-\sum_{j=1}^{n} C_{ij}\, l_{\alpha+j}}{l_{\alpha+i}}$$
$$i = 1,2,3,\ldots n$$

(27)

We can then expand (27) to have

$$\mu_x = -\left[\frac{C_{i1}l_{\alpha+1} + C_{i2}l_{\alpha+2} + \ldots + C_{in}}{l_{\alpha+i}}\right]$$

(28)

Take

$$if\ n = 5, \quad i = 3, \quad then\ \alpha = x-3$$
$$if\ n = 5 \quad i = 2, \quad then\ \alpha = x-2$$

(29)

$$C_{i1} = \sum_{\substack{k=1 \\ k\neq i}}^{n}\left[\frac{1}{x_i - x_k}\right]$$

(30)

n must be greater than 2. $n \geq 3$

C_{11} *where* $i=1,\ j=1,\ n=3, k\neq 1$

$$C_{11}=\frac{1}{x_1-x_2}+\frac{1}{x_1-x_3}$$

(31)

$$C_{11}=\ \frac{1}{1-2}+\frac{1}{1-3}=\frac{1}{-1}+\frac{1}{-2}=-1-\frac{1}{2}=\frac{-3}{2}$$

(32)

$$C_{ij}=\left(\frac{1}{x_j-x_i}\right)\prod_{\substack{k=1\\ i\neq i\\ k\neq j\\ i\neq j}}^{n}\left(\frac{x_i-x_k}{x_j-x_k}\right)$$

(33)

for $i=1,\ j=2$

$$C_{12}=\left(\frac{1}{x_2-x_1}\right)\prod_{\substack{k=1\\ k\neq 1\\ k\neq 2\\ 1\neq 2}}^{3}\left(\frac{x_1-x_2}{x_2-x_1}\right)$$

(34)

$$C_{12}=\left(\frac{1}{x_2-x_1}\right)\left[\frac{x_1-x_3}{x_2-x_3}\right]=\frac{1}{2-1}\left[\frac{1-3}{2-3}\right]=\frac{1}{1}\left[\frac{-2}{-1}\right]=2$$

(35)

$$C_{13}=\left(\frac{1}{x_3-x_1}\right)\prod_{\substack{k=1\\ k\neq 1\\ k\neq 3\\ 1\neq 3}}^{3}\left[\frac{x_1-x_k}{x_3-x_k}\right]$$

(36)

$$C_{13} = \frac{1}{x_3 - x_1} \left[\frac{x_1 - x_2}{x_3 - x_2} \right] = \frac{1}{3-1}\left(\frac{1-2}{3-2} \right) = \frac{1}{2}\left(\frac{-1}{1} \right) = \frac{-1}{2}$$

(37)

$$C_{21} = \frac{1}{x_1 - x_2} \left[\prod_{\substack{k=1 \\ k \neq 2 \\ k \neq 1 \\ 1 \neq 2}}^{3} \left(\frac{x_2 - x_k}{x_1 - x_k} \right) \right]$$

(38)

$$C_{21} = \frac{1}{x_1 - x_2}\left(\frac{x_2 - x_3}{x_1 - x_3} \right) = \frac{1}{-1}\left(\frac{2-3}{1-3} \right) = (-1)\frac{-1}{-2} = \frac{-1}{2}$$

(39)

$$C_{22} = \sum_{\substack{k=1 \\ k \neq 2}}^{n} \left(\frac{1}{x_2 - x_k} \right)$$

$i = 2, \quad j = 2, \quad n = 3 \quad k \neq 2$

(40)

$$C_{22} = \frac{1}{x_2 - x_1} + \frac{1}{x_2 - x_3} = \frac{1}{2-1} + \frac{1}{2-3} = \frac{1}{1} + \frac{1}{-1} = 0$$

(41)

$$C_{23} = \frac{1}{x_3 - x_2}\left[\prod_{\substack{k=1 \\ k\neq 2 \\ k\neq 3 \\ 2\neq 3}}^{3}\left(\frac{x_2 - x_k}{x_3 - x_k}\right)\right]$$

(42)

$$C_{23} = \frac{1}{x_3 - x_2}\left[\frac{x_2 - x_1}{x_3 - x_1}\right] = \left(\frac{1}{3-2}\right)\left(\frac{2-1}{3-1}\right) = \frac{1}{1}\left(\frac{1}{2}\right) = \frac{1}{2}$$

(43)

$$C_{31} = \frac{1}{x_1 - x_3}\left[\prod_{\substack{k=1 \\ k\neq 3 \\ k\neq 1 \\ 3\neq 1}}^{3}\left(\frac{x_3 - x_k}{x_1 - x_k}\right)\right]$$

(44)

$$C_{31} = \frac{1}{x_1 - x_3}\left(\frac{x_3 - x_2}{x_1 - x_2}\right) = \frac{1}{-2}\left(\frac{1}{-1}\right) = \frac{1}{2}$$

(45)

$$C_{32} = \frac{1}{x_2 - x_3}\left(\frac{x_3 - x_1}{x_2 - x_1}\right)$$

(46)

$$C_{32} = \frac{1}{-1}\left(\frac{3-1}{2-1}\right) = -1\left(\frac{2}{1}\right) = -2$$

(47)

$$C_{33} = \frac{1}{x_3 - x_1} + \frac{1}{x_3 - x_2} = \frac{1}{2} + \frac{1}{1} = 1\tfrac{1}{2} = \frac{3}{2}$$

(48)

$$C_{ij} = \begin{pmatrix} -3 & 4 & -1 \\ -1 & 0 & 1 \\ 1 & -4 & 3 \end{pmatrix}$$

(49)

$$\mu_x = \frac{-\sum_{j=1}^{n} C_{ij}\, l_{\alpha+j}}{l_{\alpha+i}}$$

$$i = 1, 2, 3, \ldots n$$

(50)

Model 1

McCutcheon (1983) obtained the mortality matrix as

$$c_{ij} = \begin{pmatrix} -25 & 48 & -36 & 16 & -3 \\ -3 & -10 & 18 & -6 & 1 \\ 1 & -8 & 0 & 8 & -1 \end{pmatrix}$$

(51)

$$\alpha = x - 1$$

$$\mu_{x-1+i} = -\sum_{j=1}^{5} C_{ij} l_{x-1+j}$$

(52)

$$\mu_{x-1++1} = \frac{-1}{l_x}\left[\sum_{j=1}^{5} C_{ij} l_{x-1+j}\right]$$

(53)

$$\mu_x = \frac{-1}{l_x}\left[\frac{-25}{12} l_x + \frac{48}{12} l_{x+1} - \frac{36}{12} l_{x+2} + \frac{16}{12} l_{x+3} - \frac{3}{12} l_{x+4}\right]$$

(54)

$$\mu_x = \frac{1}{l_x}\left(\frac{25}{12} l_x - \frac{48}{12} l_{x+1} + \frac{36}{12} l_{x+2} - \frac{16}{12} l_{x+3} + \frac{3}{12} l_{x+4}\right)$$

(55)

$$\mu_{x+\xi} = \frac{1}{l_{x+\xi}}\left(\frac{25}{12} l_{x+\xi} - \frac{48}{12} l_{x+\xi+1} + \frac{36}{12} l_{x+\xi+2} - \frac{16}{12} l_{x+\xi+3} + \frac{3}{12} l_{x+\xi+4}\right)$$

(55)

$${}_{\xi}p_x = e^{-\int_0^{\xi} \mu_{x+t} dt}$$

(55a)

$$ {}_{\xi}p_x = e^{-\int_0^{\xi} \frac{1}{l_{x+\xi}}\left(\frac{25}{12}l_{x+s}-\frac{48}{12}l_{x+s+1}+\frac{36}{12}l_{x+s+2}-\frac{16}{12}l_{x+s+3}+\frac{3}{12}l_{x+s+4}\right)ds} $$

(55b

Model 2

$$ i = 2 \ , \quad n = 5 $$

$$ \alpha = x - 2 $$

$$ \mu_{x-2+i} = \frac{-1}{l_x}\left[\sum_{j=1}^{5} C_{2j} l_{x-2+j}\right] $$

(56)

$$ \mu_x = \frac{-1}{l_x}\left[C_{21}l_{x-1} + C_{22}l_x + C_{23}l_{x+1} + C_{24}l_{x+2} + C_{25}l_{x+3}\right] $$

(57)

$$ \mu_x = \frac{-1}{l_x}\left[\frac{-3}{12}l_{x-1} - \frac{10}{12}l_x + \frac{18}{12}l_{x+1} - \frac{6}{12}l_{x+2} + \frac{1}{12}l_{x+3}\right] $$

(58)

$$ \mu_{x+\xi} = \frac{1}{l_{x+\xi}}\left[\frac{3}{12}l_{x+\xi-1} + \frac{10}{12}l_{x+\xi} - \frac{18}{12}l_{x+\xi+1} + \frac{6}{12}l_{x+\xi+2} - \frac{1}{12}l_{x+\xi+3}\right] $$

(59)

$$ {}_{\xi}p_x = e^{-\int_0^{\xi} \frac{1}{l_{x+s}}\left[\frac{3}{12}l_{x+s-1}+\frac{10}{12}l_{x+s}-\frac{18}{12}l_{x+s+1}+\frac{6}{12}l_{x+s+2}-\frac{1}{12}l_{x+s+3}\right]ds} $$

(55b)

Model 3

$$ i = 3, \quad n = 5, \quad \alpha = x - 3 $$

$$ \mu_{x-3+i} = \frac{-\sum_{j=1}^{n} C_{ij} l_{\alpha+j}}{l_{\alpha+i}} $$

(60)

$$\mu_x = \frac{-1}{l_x}\left[\sum_{j=1}^{5} C_{3j} l_{x-3+j}\right]$$

(61)

$$\mu_x = \frac{-1}{l_x}\left[C_{31} l_{x-2} + C_{32} l_{x-1} + C_{33} l_x + C_{34} l_{x+1} + C_{35} l_{x+2}\right]$$

(62)

$$\mu_x = \frac{-1}{l_x}\left[\frac{1}{12}\times l_{x-2} - \frac{8}{12} l_{x-1} + \frac{0}{12}\times l_x + \frac{8}{12} l_{x+1} - \frac{1}{12} l_{x+2}\right]$$

(63)

$$\mu_x = \frac{1}{l_x}\left[-\frac{1}{12} l_{x-2} + \frac{8}{12} l_{x-1} - \frac{8}{12} l_{x+1} + \frac{1}{12} l_{x+2}\right]$$

(64)

$$\mu_{x+\xi} = \frac{1}{l_{x+\xi}}\left[-\frac{1}{12} l_{x+\xi-2} + \frac{8}{12} l_{x+\xi-1} - \frac{8}{12} l_{x+\xi+1} + \frac{1}{12} l_{x+\xi+2}\right]$$

(64)

$${}_{\xi}p_x = e^{-\int_0^{\xi} \frac{1}{l_{x+s}}\left[-\frac{1}{12} l_{x+s-2} + \frac{8}{12} l_{x+s-1} - \frac{8}{12} l_{x+s+1} + \frac{1}{12} l_{x+s+2}\right] ds}$$

(65)

Presentation of Results

Table 1: (Model 1)

x	l_x	μ_x	$l_x\mu_x$
0	1000000	0.012232	12232
1	993887	0.000465	462
2	993467	0.000382	380
3	993126	0.000308	306
4	992853	0.000245	243
5	992634	0.000199	198
6	992454	0.000165	164
7	992300	0.000146	145
8	992162	0.000133	132
9	992034	0.000125	124
10	991910	0.000126	125
11	991782	0.000134	133
12	991640	0.000156	155
13	991469	0.000197	195
14	991248	0.000258	256
15	990948	0.000356	353
16	990535	0.000485	480
17	989983	0.000628	622
18	989281	0.000785	777
19	988440	0.000903	893
20	987498	0.000997	985
21	986499	0.001019	1005
22	985491	0.001021	1006
23	984501	0.000986	971
24	983553	0.000940	925
25	982657	0.000884	869
26	981816	0.000831	816
27	981023	0.000787	772
28	980265	0.000763	748
29	979528	0.000745	730
30	978799	0.000745	729
31	978063	0.000760	743

Table 1: (Model 1) – Continued

x	l_x	μ_x	$l_x\mu_x$
32	977311	0.000781	763
33	976538	0.000799	780
34	975738	0.000842	822
35	974903	0.000869	847
36	974031	0.000922	898
37	973110	0.000971	945
38	972132	0.001043	1014
39	971079	0.001128	1095
40	969933	0.001238	1201
41	968671	0.001370	1327
42	967269	0.001534	1484
43	965699	0.001723	1664
44	963929	0.001954	1884
45	961922	0.002219	2135
46	959648	0.002515	2414
47	957087	0.002826	2705
48	954232	0.003149	3005
49	951081	0.003468	3298
50	947629	0.003811	3611
51	943856	0.004178	3943
52	939731	0.004590	4313
53	935209	0.005067	4739
54	930244	0.005587	5197
55	924796	0.006170	5706
56	918822	0.006795	6243
57	912283	0.007497	6839
58	905138	0.008232	7451
59	897351	0.009055	8126
60	888867	0.009956	8850
61	979619	0.010988	10764
62	869500	0.012200	10608
63	858355	0.013667	11731
64	845970	0.015482	13097

Table 1: (Model 1) – Continued

x	l_x	μ_x	$l_x\mu_x$
65	932083	0.017708	16505
66	816413	0.020403	16657
67	798694	0.023561	18818
69	756335	0.031238	23626
70	731511	0.035568	26018
71	704285	0.040172	28293
72	674789	0.045416	30646
73	643346	0.050062	32207
74	610419	0.055076	33619
75	576168	0.060521	34870
76	540747	0.066514	35967
77	504283	0.073279	36953
78	466885	0.081019	37827
79	428691	0.089875	38529
80	389904	0.100002	38991
81	350812	0.111482	39109
82	311804	0.124459	38807
83	273364	0.138889	37967
84	236050	0.154856	36554
85	200433	0.172499	34574
86	167061	0.191962	32069
87	136432	0.213353	29108
88	108965	0.236552	25776
89	84962	0.261473	22215
90	64565	0.288082	18600
91	47742	0.316252	15099
92	34298	0.345861	11862
93	23903	0.377160	9015
94	16137	0.409272	6604
95	10540	0.443398	4673
96	6650	0.477882	3178
97	4048	0.514863	2084
98	2372	0.552522	1311
99	1335	0.595443	795

Table 1: (Model 1) – Continued

x	l_x	μ_x	$l_x\mu_x$
100	719	0.637228	458
101	370	0.684459	253
102	181	0.738029	134
103	84	0.767857	64
104	37	0.882883	33
105	15	0.794444	12
106	6	1.250000	8
107	2	0.083333	0
108	1	2.083333	2

Figure 1a: Survival Curve

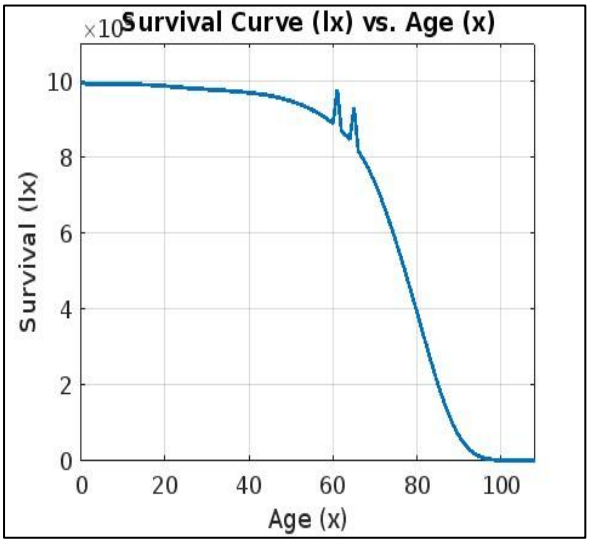

Fig 1b: mortality Curve

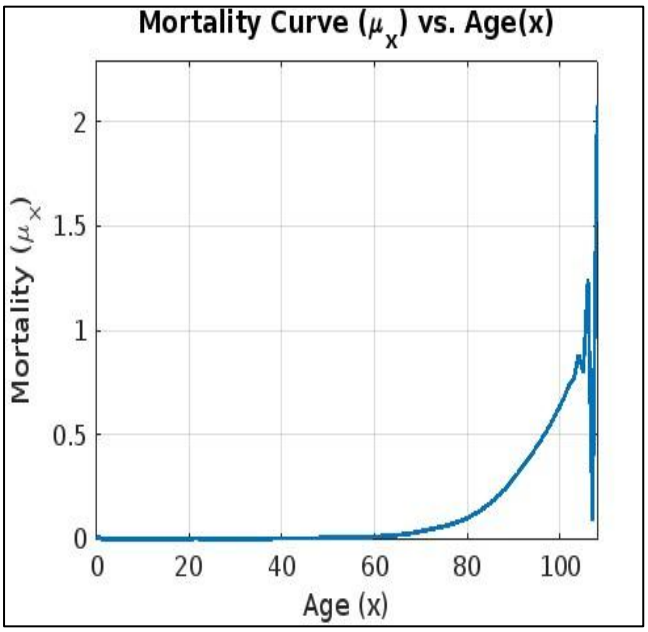

Fig 1c: Curve of death

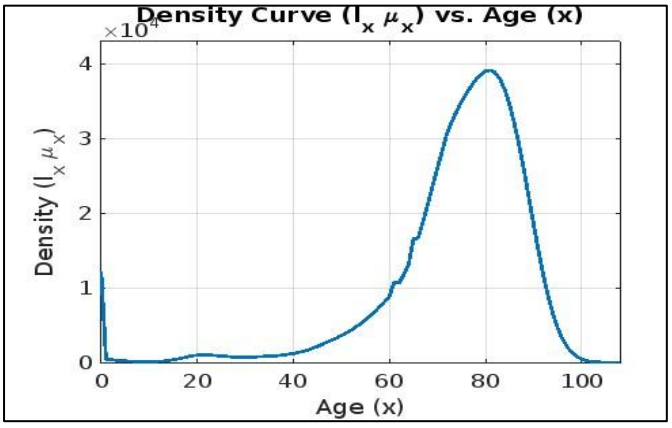

Fig 1d: Surface plots

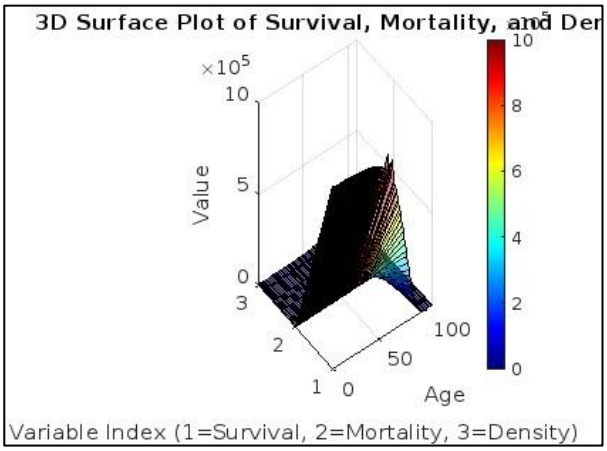

Table 2: (Model 2)

x	l_x	μ_x	$l_x\mu_x$
0	1000000	0.00188	1875
1	993887	0.00038	379
2	993467	0.00031	305
3	993126	0.00025	243
4	992853	0.0002	198
5	992634	0.00017	165
6	992454	0.00015	145
7	992300	0.00013	132
8	992162	0.00013	125
9	992034	0.00013	125
10	991910	0.00013	133
11	991782	0.00016	154
12	991640	0.00019	191
13	991469	0.00026	254
14	991248	0.00035	351
15	990948	0.00048	479
16	990535	0.00063	627
17	989983	0.00079	778

Table 2: (Model 2) – Continued

x	l_x	μ_x	$l_x\mu_x$
18	989281	0.00091	899
19	988440	0.00099	982
20	987498	0.00102	1009
21	986499	0.00102	1005
22	985491	0.00099	973
23	984501	0.00094	924
24	983553	0.00088	868
25	982657	0.00083	816
26	981816	0.00079	774
27	981023	0.00076	747
28	980265	0.00075	730
29	979528	0.00075	731
30	978799	0.00076	744
31	978063	0.00078	762
32	977311	0.0008	786
33	976538	0.00084	818
34	975738	0.00087	852
35	974903	0.00092	897
36	974031	0.00097	948
37	973110	0.00104	1014
38	972132	0.00113	1097
39	971079	0.00124	1202
40	969933	0.00137	1330
41	968671	0.00153	1483
42	967269	0.00172	1666
43	965699	0.00195	1886
44	963929	0.00222	2141
45	961922	0.00252	2422
46	959648	0.00283	2715
47	957087	0.00315	3012
48	954232	0.00347	3310
49	951081	0.00381	3622
50	947629	0.00418	3957

Table 2: (Model 2) – Continued

x	l_x	μ_x	$l_x\mu_x$
51	943856	0.00459	4334
52	939731	0.00507	4760
53	935209	0.00559	5227
54	930244	0.00617	5739
55	924796	0.0068	6290
56	918822	0.0075	6887
57	912283	0.00824	7516
58	905138	0.00906	8198
59	897351	0.00996	8937
60	888867	0.01099	9764
61	979619	0.01219	11943
62	869500	0.01366	11875
63	858355	0.01547	13280
64	845970	0.0177	14975
65	932083	0.0204	19013
66	816413	0.02356	19236
67	798694	0.02718	21708
68	778714	0.03121	24300
69	756335	0.03559	26914
70	731511	0.04033	29501
71	704285	0.04531	31908
72	674789	0.05007	33787
73	643346	0.05507	35430
74	610419	0.0605	36931
75	576168	0.0665	38313
76	540747	0.07327	39621
77	504283	0.08101	40852
78	466885	0.08988	41963
79	428691	0.10002	42876
80	389904	0.11153	43484
81	350812	0.12449	43672
82	311804	0.13891	43314
83	273364	0.15489	42341

Table 2: (Model 2) – Continued

x	l_x	μ_x	$l_x\mu_x$
84	236050	0.17255	40730
85	200433	0.19203	38488
86	167061	0.21338	35647
87	136432	0.23653	32270
88	108965	0.26139	28482
89	84962	0.28791	24461
90	64565	0.31599	20402
91	47742	0.34558	16499
92	34298	0.37669	12920
93	23903	0.40906	9778
94	16137	0.44297	7148
95	10540	0.47811	5039
96	6650	0.51517	3426
97	4048	0.55431	2244
98	2372	0.59694	1416
99	1335	0.64175	857
100	719	0.69054	496
101	370	0.74355	275
102	181	0.79464	144
103	84	0.86937	73
104	37	0.91111	34
105	15	1.04167	16
106	6	0.83333	5
107	2	1.33333	3
108	1	-	0

Figure 2a: Survival function

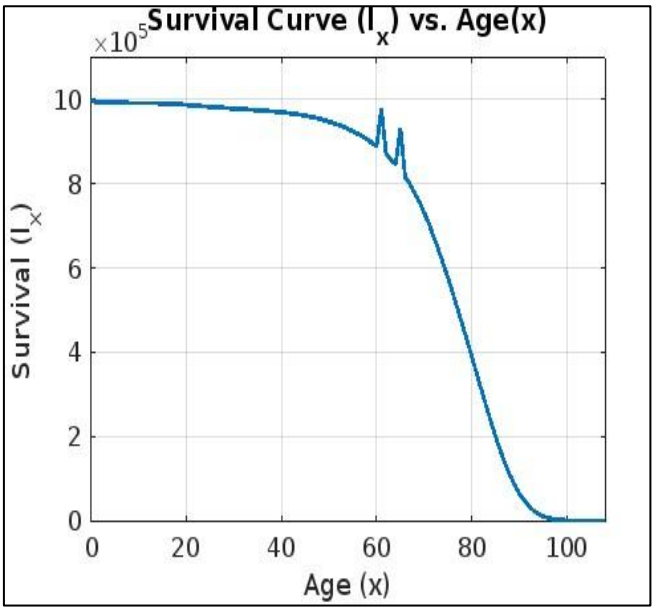

Figure 2b: mortality function

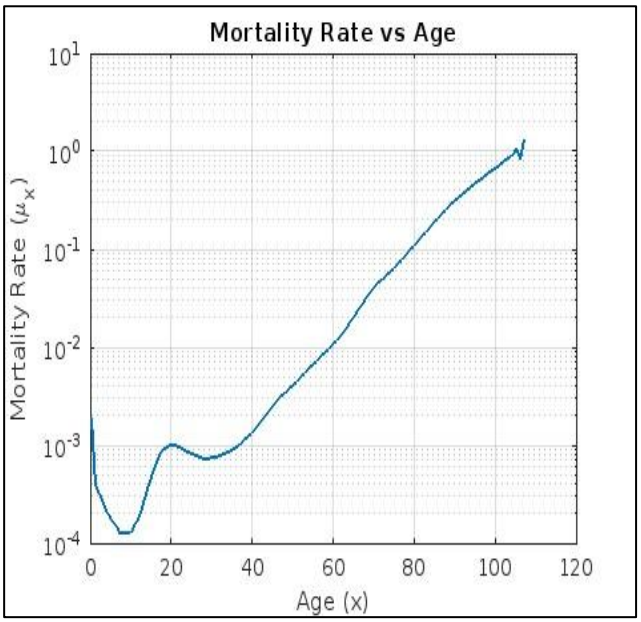

Figure 2c: Density function

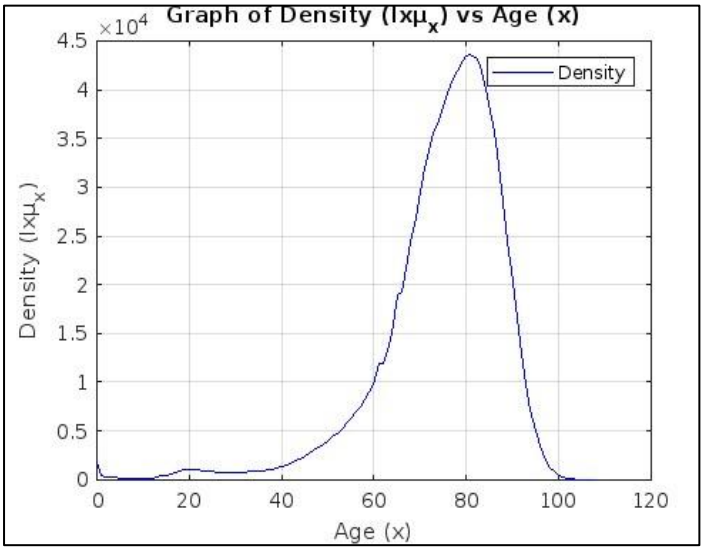

Figure 2d: Surface Plots

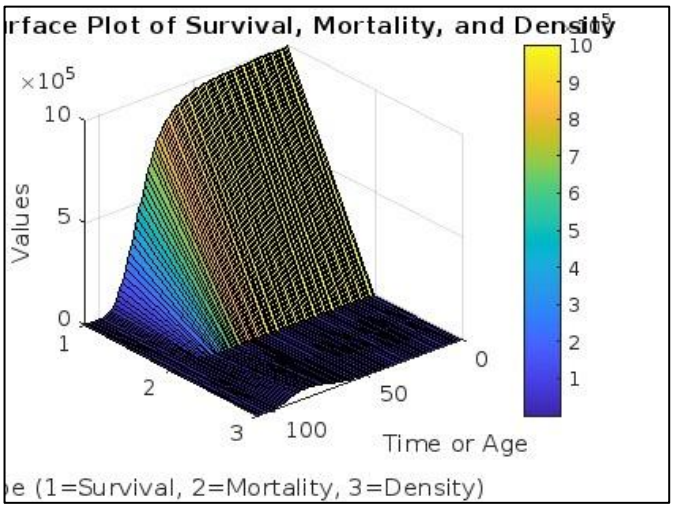

Table 3: (Model 3)

x	l_x	μ_x	$l_x\mu_x$
0	1000000	-	100000
1	993887	0.000310	308
2	993467	0.000250	248
3	993126	0.000200	199
4	992853	0.000170	169
5	992634	0.000150	149
6	992454	0.000130	129
7	992300	0.000130	129
8	992162	0.000130	129
9	992034	0.000130	129
10	991910	0.000150	149
11	991782	0.000190	188
12	991640	0.000260	258
13	991469	0.000350	347
14	991248	0.000480	476
15	990948	0.000630	624
16	990535	0.000780	773
17	989983	0.000910	901
18	989281	0.000990	979
19	988440	0.001020	1008
20	987498	0.001020	1007
21	986499	0.000990	977
22	985491	0.000940	926
23	984501	0.000880	866
24	983553	0.000830	816
25	982657	0.000790	776
26	981816	0.000760	746
27	981023	0.000750	736
28	980265	0.000750	735
29	979528	0.000760	744
30	978799	0.000780	763
31	978063	0.000800	782

Table 3: (Model 3) – Continued

x	l_x	μ_x	$l_x\mu_x$
32	977311	0.000840	821
33	976538	0.000870	850
34	975738	0.000920	898
35	974903	0.000970	946
36	974031	0.001040	1013
37	973110	0.001130	1100
38	972132	0.001240	1205
39	971079	0.001370	1330
40	969933	0.001530	1484
41	968671	0.001720	1666
42	967269	0.001950	1886
43	965699	0.002220	2144
44	963929	0.002520	2429
45	961922	0.002830	2722
46	959648	0.003150	3023
47	957087	0.003470	3321
48	954232	0.003810	3636
49	951081	0.004180	3976
50	947629	0.004590	4350
51	943856	0.005060	4776
52	939731	0.005590	5253
53	935209	0.006170	5770
54	930244	0.006800	6326
55	924796	0.007490	6927
56	918822	0.008240	7571
57	912283	0.009050	8256
58	905138	0.009960	9015
59	897351	0.010980	9853
60	888867	0.012190	10835
61	979619	0.013660	13382
62	869500	0.015470	13451
63	858355	0.017710	15201

Table 3: (Model 3) – Continued

x	l_x	μ_x	$l_x\mu_x$
64	845970	0.020400	17258
65	932083	0.023560	21960
66	816413	0.027180	22190
67	798694	0.031200	24919
68	778714	0.035600	27722
69	756335	0.040320	30495
70	731511	0.045250	33101
71	704285	0.050110	35292
72	674789	0.055070	37161
73	643346	0.060500	38922
74	610419	0.066500	40593
75	576168	0.073280	42222
76	540747	0.081010	43806
77	504283	0.089880	45325
78	466885	0.100010	46693
79	428691	0.111520	47808
80	389904	0.124470	48531
81	350812	0.138900	48728
82	311804	0.154880	48292
83	273364	0.172530	47163
84	236050	0.192010	45324
85	200433	0.213350	42762
86	167061	0.236520	39513
87	136432	0.261400	35663
88	108965	0.287940	31375
89	84962	0.316070	26854
90	64565	0.345710	22321
91	47742	0.376820	17990
92	34298	0.409290	14038
93	23903	0.443080	10591
94	16137	0.478330	7719
95	10540	0.515050	5429

Table 3: (Model 3) – Continued

x	l_x	μ_x	$l_x\mu_x$
96	6650	0.554140	3685
97	4048	0.595880	2412
98	2372	0.640820	1520
99	1335	0.687610	918
100	719	0.739410	532
101	370	0.790670	293
102	181	0.849100	154
103	84	0.922220	77
104	37	0.944440	35
105	15	1.041670	16
106	6	0.833330	5
107	2	-	2
108	1	-	1

Figure 3a: Survival function

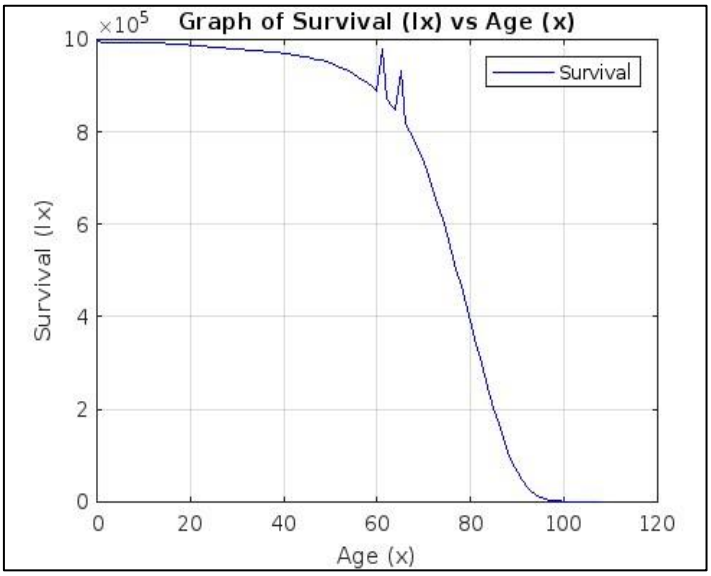

Figure 3b: Mortality function

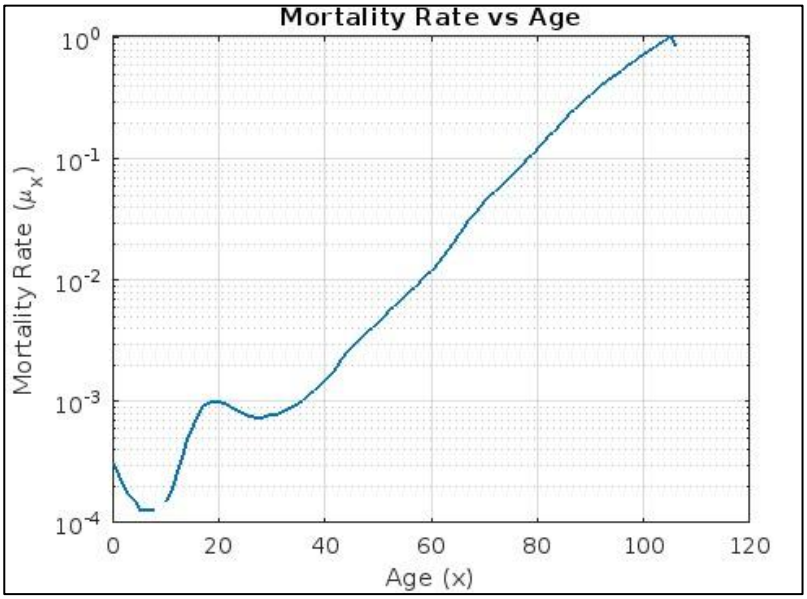

Fig 3c: Density function

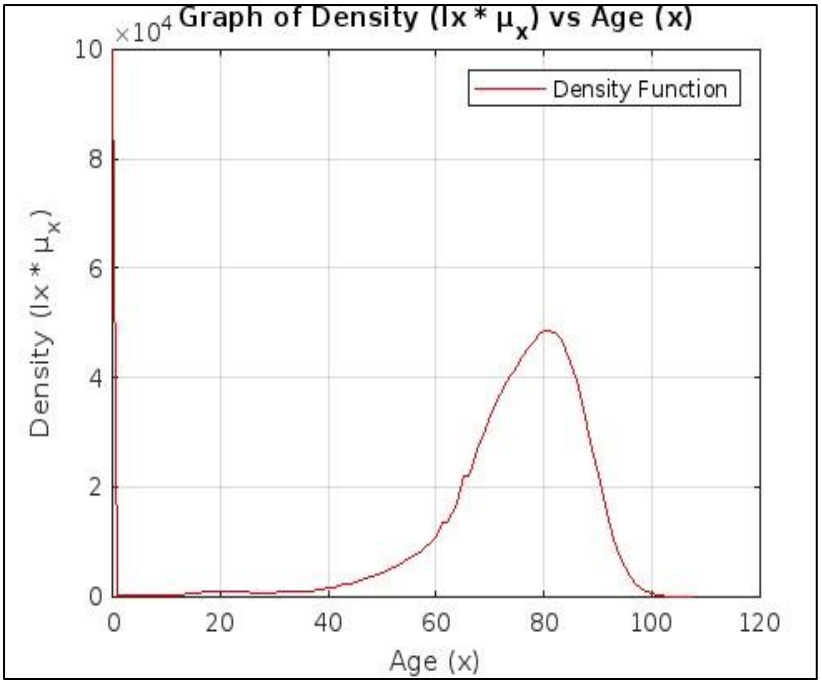

Fig 3d: Surface Plots

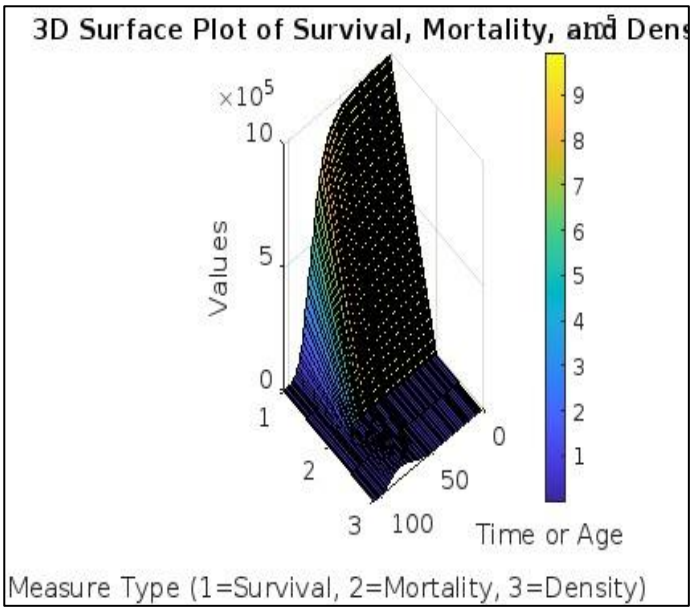

Discussion

In Tables 1 and 2, the force of mortality μ_x is clearly defined at perinatality $x=0$ and consequently, the intensities μ_0 can be captured. In Figures 1, it is observed that μ_x displays a continuously smooth curve but seems to cluster around the neighbourhood of age 105 suggesting more deaths than elsewhere while the survival curves in Figures 1a, 2a, 3a exhibit kinks within the interval $60 \le x \le 70$. Although, the survival function in Figure 2a kinks within $60 \le x \le 70$, the trajectory of the mortality function increases continuously in figure 2. In tables 3, the instantaneous death rate μ_x is not defined at $x=0$ and hence the intensities μ_0 cannot be captured. In this case, it is clear that the estimation of μ_x is by far a difficult problem where part of the difficulty is the estimation of μ_0 at initial age when the only information given is l_x. The mortality at age zero μ_0 is defined in the Gompertz's law but the law is not designed to measure mortality at age zero in practice as mortality

cannot increase exponentially during infancy. In order to address the problems connected with intractable μ_0 in equation (64) at age 0 in Tables 3 and compare with Gompertz's law $\mu_x = BC^x$, the following close form model are analytically developed.

$$l_1 = l_0 + \Delta l_0' + \frac{\Delta^2}{2} l'' + \frac{\Delta^3}{6} l_0''' + \ldots$$

(66)

$$l_2 = l_0 + 2\Delta l_0' + 2\Delta^2 l_0'' + \frac{4\Delta^3}{3} l_0''' + \ldots$$

(67)

We apply linear combination of l_0, l_1, l_2 which gives l_0'

$Al_0 + Bl_1 + Cl_2 \to l_0'(only)$. Substitute the Taylor series expansion above yields

$$Al_0 + B\left(l_0 + \Delta l_0' + \frac{\Delta^2}{2} l'' + \frac{\Delta^3}{6} l_0''' + \ldots \right) + C\left(l_0 + 2\Delta l_0' + 2\Delta^2 l_0'' + \frac{4\Delta^3}{3} l_0''' + \ldots \right) = l_0'$$

(68)

We then extract the coefficients according of l_0 and its derivatives.

$$l_0 : A + B + C$$

$$l_0' : B\Delta + 2C\Delta$$

$$l_0'' : \frac{B\Delta^2}{2} + 2C\Delta^2$$

$$l_0''' : \frac{B\Delta^3}{6} + \frac{4C\Delta^3}{3}$$

(69)

Now eliminate all terms except the one with l_0' and hence solve

$$A + B + C = 0$$

$$B\Delta + 2C\Delta = 1$$

$$\frac{B}{2} + 2C = 0$$

(70)

$$\frac{B}{2} + 2C = 0 \Rightarrow B = -4C$$

(71)

$$(-4C)\Delta + 2C\Delta = 1 \Rightarrow C = \frac{-1}{2\Delta}$$

(72)

$$B = -4C = \frac{2}{\Delta}$$

(73)

$$A = -B - C = \frac{-2}{\Delta} + \frac{1}{2\Delta} = \frac{-3}{2\Delta}$$

(74)

$$l_0' = Al_0 + Bl_1 + Cl_2 = \frac{-3}{2\Delta} l_0 + \frac{2}{\Delta} l_1 - \frac{1}{2\Delta} l_2$$

(75)

Factor out $\frac{1}{2\Delta}$

$$l_0' = \frac{1}{2\Delta}(-3l_0 + 4l_1 - l_2)$$

(76)

$$\mu_0 = -\frac{l_0'}{l_0} = -\frac{1}{2\Delta}(-3l_0 + 4l_1 - l_2) = \frac{1}{2\Delta l_0}(3l_0 - 4l_1 + l_2)$$

(77)

The Gompertz's law is defined for the age interval $60 \le x \le 90$ and assumes exponential increase in age at senescence. Although real-life mortality patterns in young age groups increase linearly due to external factors such as accidents, life style, environmental influences and as a result the classical Gompertz's and Makeham's laws which are dominated by the exponential term do not capture these early-life mortality trends. Of great concern in model-based mortality analysis is that the existing methods such as in Putra, Fitriyati and Mahmudi (2019) and Muzaki, Siswannah and Miasary (2020), the maximum likelihood estimation method used to estimate the parameters of the classical Makeham's law have exhibited clear limitations particularly in obtaining the ageing parameter C to conform with the globally accepted critical interval 1.08 and 1.12. A major problem with maximum likelihood method is that two parameters can influence the likelihood function which make the Jacobian columns of the Jacobian matrix to be linearly independent and hence the matrix becomes conditionally ill and hence the determinant is singular. Consequently, the parameters cannot be estimated. In the Gompertz's law, the hazard rate increases without bounds as the age $x \to \infty$.

However, depending on the degree, the polynomial-based hazard can increase, decrease or oscillate. The oscillation may be due to the Runge's phenomenon, a problem associated with polynomial based mortality modelling when kinks occur.

In Figures 1 and 2, the mortality rates exhibit wavy kinks within $105 \le x \le 113$ with a higher degree of complexity and increasing the mortality risk of shocks or idiosyncrasies at advanced ages. The wavy kinks in the curves functionally connected with a high risk of noise occurs when using the polynomials associated with high-order dimensional non-square mortality matrix to capture shocks rather than the true underlying trend. Furthermore, the kinky points may have occurred as a result of the Runge's Phenomenon associated with polynomial modelling. In Figures 1, 2 and 3, the mortality rates may be risky for extrapolation beyond approved respective ranges $105 \le x \le 113$ and $101 \le x \le 111$ of mortality data as they can behave erratically outside the fitted range. Moreover, the modal age at death can be estimated as 80 years.

Consequently, the erratic behaviour of mortality rate associated with shocks within the intervals $105 \le x \le 113$ and $101 \le x \le 111$ are susceptible to the following consequences: While polynomial-based mortality can be used for extrapolation, there's a risk that the model derived may not accurately predict long-term future mortality trends beyond the approved age, especially when the mortality pattern changes over time or in response to some health interventions such as medical advancements and health policies. As a result, the models may not capture shifts in trends caused by sudden changes in disease patterns or demographic shifts, such as a significant aging population or major public health crises. If polynomial is used for long-term mortality forecasting, then there is a significant risk of uncertainty**.**

Mortality rates can change due to shifts in medical technology, lifestyle changes and other external factors that the polynomial model may not account for. Mortality models influence important underwriting decisions, including resource allocation such as healthcare spending; public health initiatives such as anti-smoking campaigns, vaccination programs and retirement planning such as pension systems. If the model overestimates or underestimates mortality rates, it could lead to misallocation of resources. If the polynomial model fails to capture

mortality changes due to new diseases or aging populations, policymakers might fail to adequately prepare for future challenges.

Since μ_x usually varies rapidly in the interval $0 \le x \le 1$, there may not be any universally acceptable measure of μ_0. The mortality intensity μ_x demonstrates a continuously smooth curve but it is observed to kink into steps within $41 \le x \le 71$. In Tables 1, there does not seem any age where the mortality intensity $\mu_x = \mu$ is constant. The implication is that at adult ages, the risk of ageing will continuously escalate and any cause of death will increase at higher degree of intensities such that more severe ageing is caused as the force of mortality increases.

In both Tables 1 and 2, the intensities decline at age $23 \le x \le 29$ and then steadily increases while in tables 3, the intensities decline at age $23 \le x \le 33$, this result is consistent with the stylized fact that $x = 10$ is the minimum point of mortality. However, $\mu_x = \mu$ is constant within the interval $8 \le x \le 9$ and thereafter progressively increases till senescence. In Table 3, although, the mortality intensity μ_x is not both defined at age $x = 0$, it becomes constant in the age interval $6 \le x \le 9$. In this interval, this constant force of mortality can be observed from the survival probability ${}_z p_x = e^{-\int_0^z \mu dy} = e^{-\mu z}$.
Under this constant force assumption, the probability that a life survives to age $z + x$ within the age interval $6 \le x \le 9$ becomes independent of x and consequently, the remaining lifetime approaches the negative exponential distribution when the age attained increases. Since life offices need a good estimates of mortality rates to price life annuities and reverse mortgages, this may offer a conservative technique in valuating life insurance schemes and life annuities.

It is clear from the results of the computation that mortality intensities comparatively improve, best in Table 3. This may be due to the flexibility and scalability in model 3 permitting the choice of the degree of complexity in computing intensities and fitting the mortality curves with a trade-off between information requirement and accuracy. Consequently, as the subscripts i increases, the approximation obtained

improves. Recall that $\mu_x = -\frac{l'_x}{l_x}$, consequently, in Table 1, the resistance to mortality rate intensities at age x $modal\,age$ defined by $\xi = \left(\frac{1}{\mu_x}\right) = -\frac{l_x}{l'_x}$ decreases from 81.7528 at age 0 to 0.4800 at age 108. The trend changes in table 2, as ξ decreases from 533.3333 at age 0 to 0.7500 at age 107. In Table 3, ξ decreases from 3225.8065 at age 1 to 1.2000 at age 106. The resistance which could be employed in measuring life expectancy at senescent ages would stabilize as $\lim_{x\to\Omega}\left(\frac{d\xi}{dx}\right) = 0$

Conclusion

This study demonstrates the significant potential of employing a non-square matrix generated from McCutcheon's polynomial in modeling mortality rate intensity. By leveraging the polynomial's flexibility in capturing complex, age-specific mortality dynamics, the proposed model improves both the accuracy and interpretability of mortality rate predictions. The application of a non-square matrix allows for more nuanced modeling of nonlinear and time-dependent effects, which traditional square matrix approaches often overlook. Through case studies and comparative analysis, it was shown that this method enhances predictive power and provides a more adaptable framework for diverse populations. The results emphasize the value of extending classical demographic models and suggest that McCutcheon's polynomial, in its extended form, offers a promising tool for future research in mortality modeling, with implications for actuarial science, public health, and demographic forecasting. Further work can explore the integration of additional demographic factors and the refinement of the model to address specific population subsets and longitudinal data.

Applying polynomials in modeling mortality rates can be a useful approach, particularly in cases where the mortality data exhibits complex or non-linear patterns that are difficult to capture with simpler linear models. Polynomials can provide flexibility in fitting the data, making them a good tool for descriptive analysis and certain types of predictive modeling. Using historical mortality data, a polynomial model can predict

future mortality trends based on observed time patterns. For example, in countries with aging populations, a polynomial model might capture the acceleration of mortality in older age groups over time. Mortality rates can change over time due to various factors, such as improvements in healthcare, lifestyle changes, or the emergence of new diseases.

Polynomial models can be used to fit mortality trends as a function of time, particularly when there are non-linear trends**.** Polynomials can also be applied to model mortality rates in subgroups**,** such as by gender, socioeconomic status, or geographic region. These subgroups may exhibit different mortality trends, which polynomials can capture effectively.

In this paper, we have given a detailed analysis of mortality modelling based on McCutcheon's mortality polynomial matrices to explain decline in mortality. Three models were developed to that effect. All the three models yield positive mortality intensities. However, decreasing trend is observed beyond the age 10 and almost constant patterns were observed within the interval indicated across the models.

References

Ah-Khaliludin, N.I., Khalid Z.M., and AbdRahman H. 2019. On estimate of Malaysian mortality rates using interpolation methods, *Matematika: Mjiam, 35*(2), 177-186

Bolx-Postigo M., Aguero R., and Melus-Moreno J.L. 2019. An alternative procedure to obtain the mortality rate with nonlinear functions: Application to the case of the Spanish population, *Plos One, 14*(10), 1-16 https://doi.org/10.1371/journal.pone.0223789

Faraway J.J. 2016. Extending the linear model with R, $2nd$ Ed, Chapman and. Hall/CRC Kaishev V.K, Dimitrova, D.S., Haberman S and Verall R. 2016. Geometrically designed variable knot regression splines. *Computational Statistics Vol. 31*, Springer

Li H., O'Hare C., Vahid, F. 2016. A flexible functional form approach to mortality modelling: Do we need additional cohort dummies?, *Digitales Archiv*, page 1-22, doi:10.2139/ssm.2553041

McCutcheon J.J. 1983. On estimating the force of mortality. *Transaction of the Faculty of* actuaries *38* ,407-417

Oirov T., Terbish G., and Dorj N. 2021. B-spline estimation for force of mortality, *Mathematics and Statistics, 9*(5), 736-743. DOI: 10.13189/ms.2021.090513

Spreeuw J, Owadally I, Kashif M. 2022. Projecting mortality rates using a Markov chain. *Mathematics, 10*(162), 1-1